

“Observations of Solar Storms in the Outer Corona”

A. Bemporad

INAF – Turin Astronomical Observatory



SWIFF – Space Weather
Integrated Forecasting Framework



INAF – Italian National
Astrophysics Institute

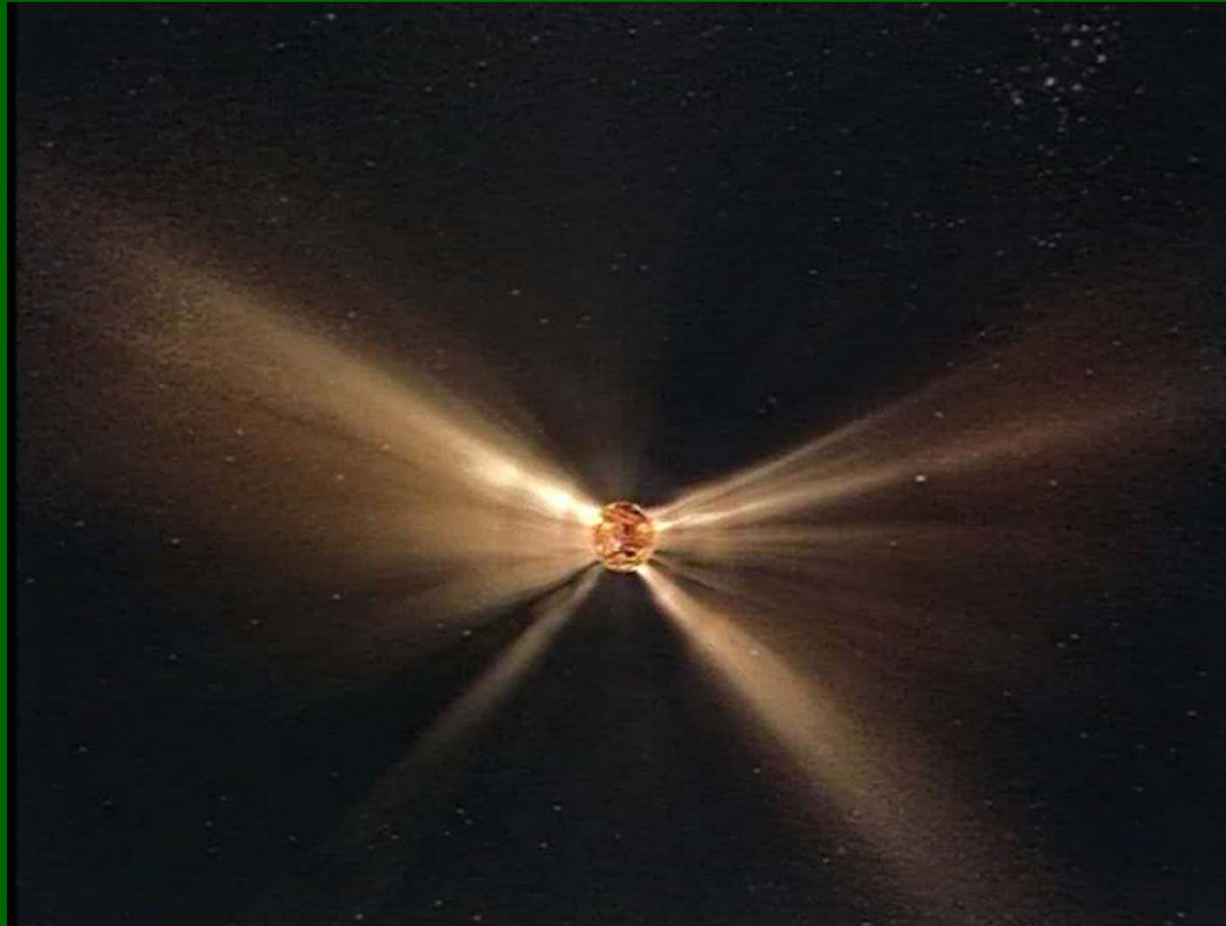


OATo – Turin Astro-
nomical Observatory

Outline

- Introduction: Coronal Mass Ejections (CMEs)
- Observations of CMEs in the outer corona:
White light, Radio, UV
- Next future
- Conclusions

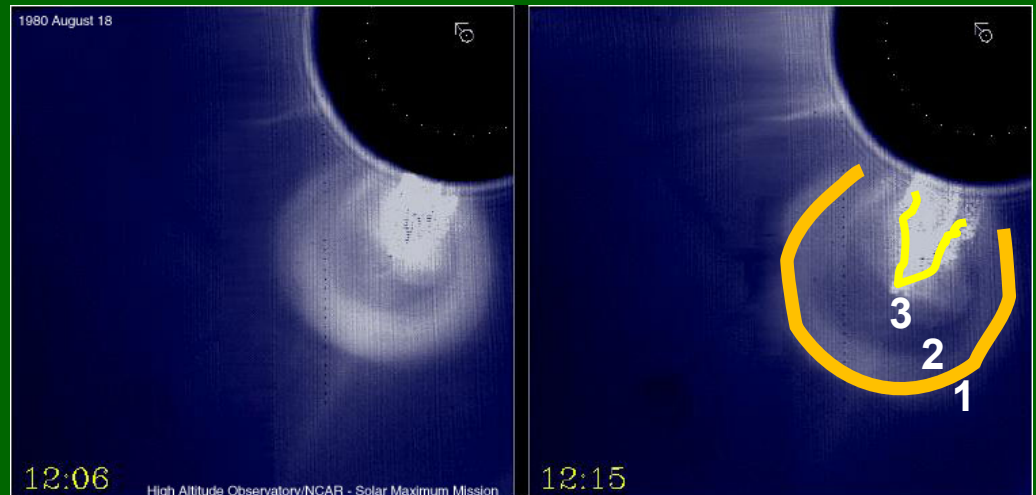
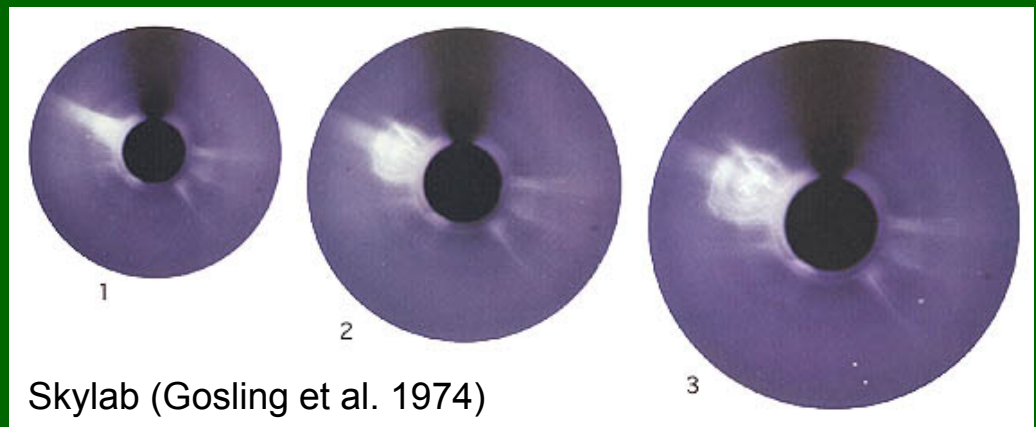
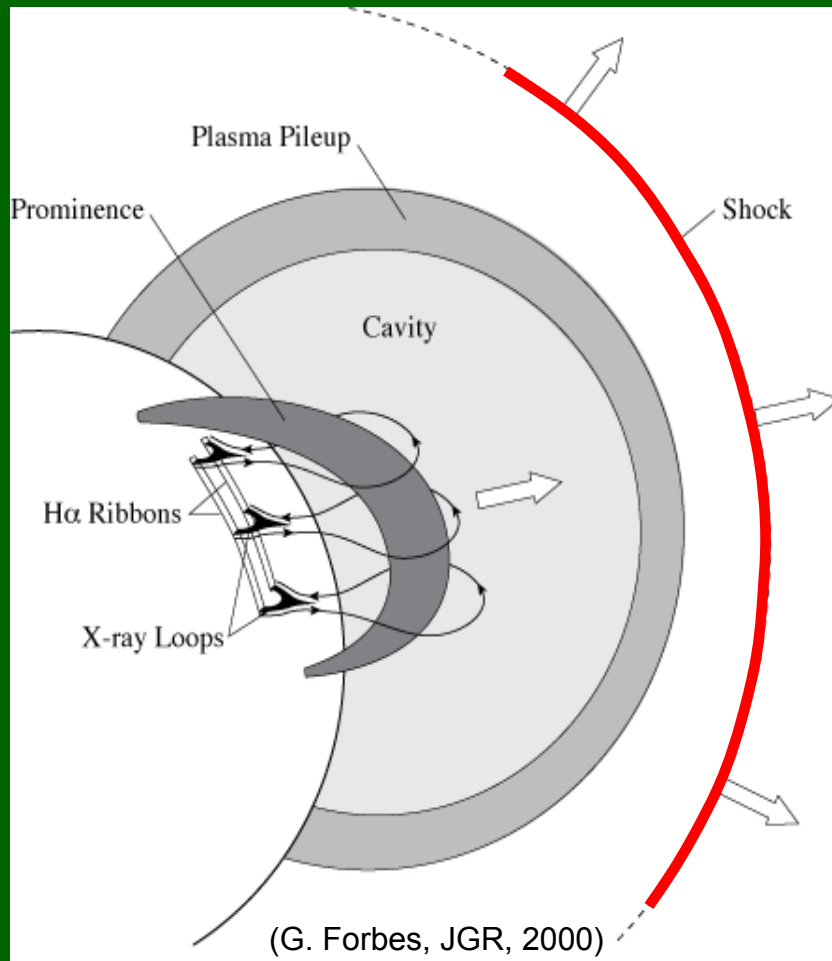
Observations of Coronal Mass Ejection (CMEs)



The Sun produces 2-4 CMEs/day during solar minima, 6-8 CMEs/day during solar maxima (Cactus catalog). A mass between $10^{13} - 10^{16}$ g is ejected at a velocity between 100-2500 km/s (Howard et al. 1985; Hundhausen, Burkepile & StCyr 1994).

Information on CMEs in the outer corona by: **remote sensing** (ground- and space-based WL coronagraphs, heliospheric imagers, radioheliographs, EUV imagers & spectrometers) and **in situ** instruments (for ICMEs).

CME morphology



Classical “3-part structure” (Hilling & Hundhausen 1985): 1) **FRONT** (=dragged coronal plasma), 2) **CAVITY** (=expanding flux tube?), 3) **CORE** (=prominence), 4) **SHOCK** → “4-part str.”

Observations demonstrate that CMEs have a variety of geometries, narrow jets, streamer blowouts, halo CMEs, etc...

CME origin

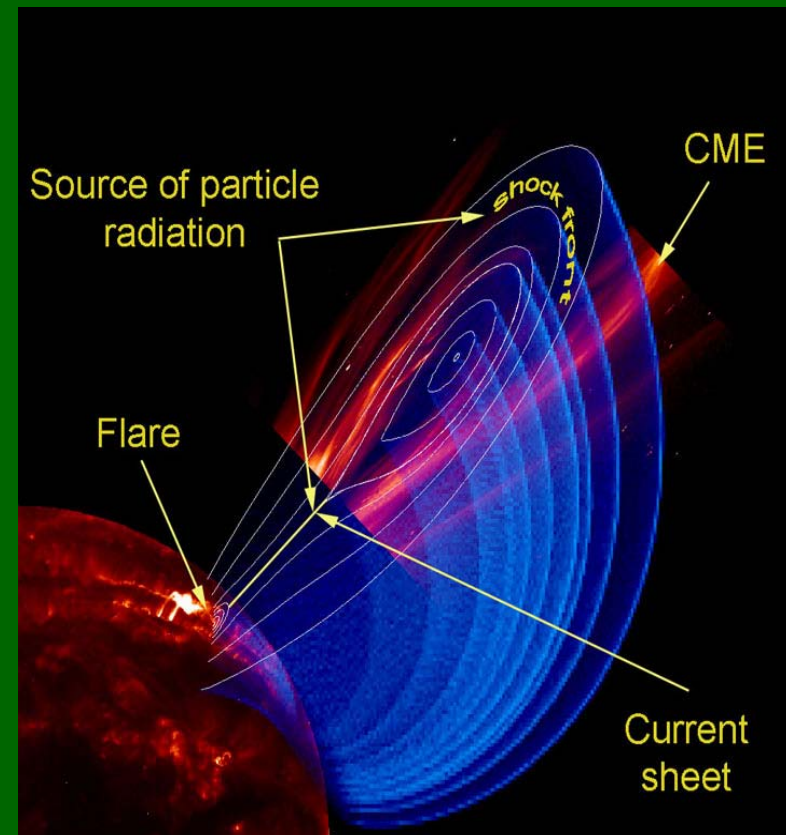
Energy requirement of a moderately large CME

Parameter	Value
Kinetic energy (CME, Prominence, & shock)	10^{32} erg
Heating & radiation	10^{32} erg
Work done against gravity	10^{32} erg
Volume involved	10^{30} cm ³
Energy density	100 erg cm ⁻³

Estimates of coronal energy sources

Form of Energy	Obs. average values	Energy density erg cm ⁻³
Kinetic ($m_p n V^2 / 2$)	$n = 10^9$ cm ⁻³ ; $V = 1$ km s ⁻¹	10^{-5}
Thermal ($2nkT$)	$T = 10^6$ K	0.2
Gravitational ($m_p n g h$)	$h = 10^5$ km	0.5
Magnetic ($B^2 / 2\mu_0$)	$B = 100$ G	400

Forbes (2000 JGR 105, 23153)



Comparison between **typical CME energy densities** and possible **coronal sources** → **required energy** from the storage and conversion of **magnetic energy** in thermal and kinetic energy. The process for energy conversion is the **magnetic reconnection**.

“STANDARD” CSHKP MODEL:

(Carmichael – Sturrok – Hirayama – Kopp – Pneumann)

- **Rising prominence** (twisted fluxtube)
- **Reconnection** → **flare**, particles acceleration, formation of hot **post-flare loops**, prominence eruption (**CME**).
- **Inflow** of high temperature plasma → footpoints heating → **H α ribbons**
- **Reconnection** → field relaxation and formation of a high temperature Current Sheet (CS)

CMEs: major open problems

Major open problems on Coronal Mass Ejections are:

- **CME origin:** how the magnetic energy is stored? How the energy release is triggered? Magnetic shearing? Flux emergence? Loss of equilibrium of flux ropes? Magnetic breakout?
- **CME 3-D structure:** hollow flux-ropes? Hemispherical shells? Expanding loops? 3D morphology is the “driver behind the development of theoretical ideas” (Thernisien et al. 2010), gives better determination of true propagation direction.
- **Energy budget** of the ejected plasma: CME eruption can dissipate a great deal of magnetic energy, but how much of this energy takes the form of radiation, thermal energy, mechanical energy, particle acceleration? Less is known about the heating of CME plasma after the initial ejection.
- **Interplanetary Evolution:** during their Interplanetary propagation CMEs are subject to a) propelling / retardind forces, b) latitudinal / longitudinal deflections, c) rotations around their vertical axis, d) plasma heating (in situ high charge states) but we don't know the physical processes responsible for these phenomena.
- **SEP acceleration:** where (shocks or flares?) and how are them accelerated?
- **Space Weather:** what determines the CME geoeffectiveness?

Which information we derived from remote sensing observations in the outer corona?

White Light observations

CME statistical studies



(Webb & Howard 2012)

Availability of coronagraphic images from space allowed for a continuous monitoring of CMEs
 → first **CME catalogues** and **statistical studies**.

Coronagraph	OSO-7	Skylab	Solwind	SMM ^a	LASCO ^b
Epoch	1971	1973–74	1979–85	1980, 84–89	1996–present
FOV (R_{\odot})	2.5–10	1.5–6	3–10	1.6–6	1.2–32
Total # CMEs	27	115	1607	1351	> 10000
Speed (km s^{-1})	–	470	460	349	489
Acceleration (m s^{-2})	–	–	–	–	–16 to +5
Width ($^{\circ}$)	–	42	43	46	47
Mass (10^{15} g ^c)	–	6.2	1.7	3.3	1.3
KE (10^{30} erg ^c)	–	–	4.3	8.0	2.0
Mech. E (10^{30} erg ^c)	–	–	–	–	4.2

CME catalogs:

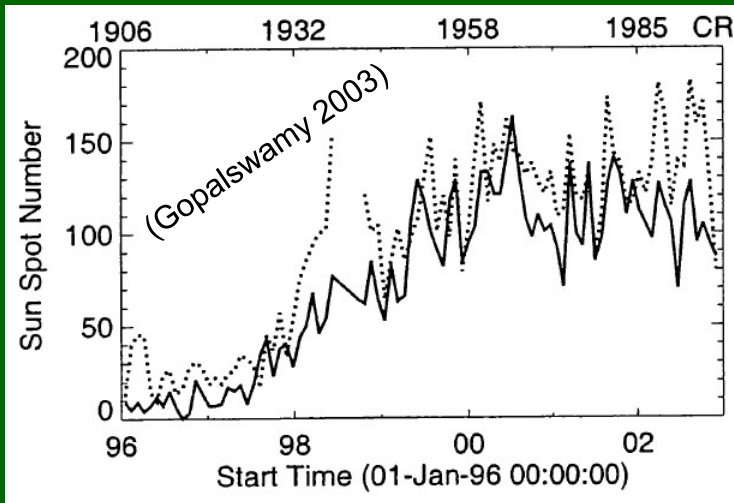
- *Visual inspection of data* → CDAW (Yashiro et al. 2004; Gopalswamy et al. 2005)
- *Automatic detection* → CACTus (Robbrecht et al. 2009), SEEDS (Olmedo et al. 2008), ARTEMIS (Boursier et al. 2009).

Differences among different catalogs:

- CACTus automatically identify more narrow ($<20^{\circ}$) events (missed at solar max)
- CDAW fast ($v > 1000$ km/s) CMEs are wider and originate from lower latitudes
- Automatic catalogs not always identify wide/halo CMEs

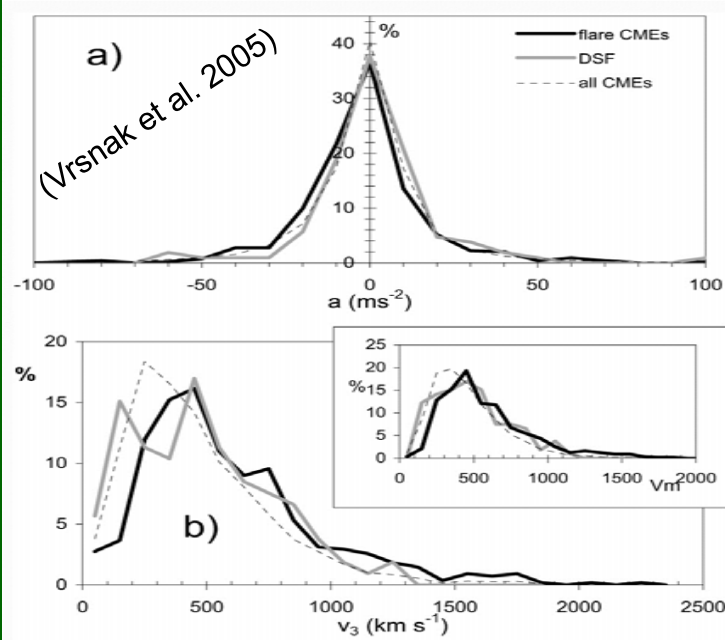
Not a general consensus on the **standard definition of a “CME”**

Some results from statistical studies



CME rate: follows the solar cycle (Gopalswamy et al. 2003, 2005, 2006), CME rate and sunspot number have a linear relationship (Webb & Howard 1994; Robbrecht 2009)

CME latitude / width: around the equator at solar min, over all latitudes at solar max (Gopalswamy et al. 2004, 2010) → CME match more the distribution of prominences/ streamers than that of ARs (first Hundhausen 1993 with SMM). Wider CMEs are faster (confirmed by STEREO, Howard et al. 2008)



CME-flare: flare-related CMEs are faster, good correlation CME speed vs X-ray flux (Moon et al. 2002; Yashiro & Gopalswamy 2008); kinetic energy distribution has power law index (-1; Vourlidas et al. 2002) ≠ than that for flares (-2; Yashiro et al. 2006).

Flare and non-flare CMEs are very similar (Vrsnak et al. 2005) → 2 dynamical classes (gradual & impulsive) of CMEs exist?

CME 3-D structure

Single view-point: degree of polarization of Thomson-scattering depends on scattering angle (Billings 1966) → single view-point pB-tB images contain information on CME 3-D structure → **polarization ratio technique** (Crifo et al. 1983 - validated with STEREO Moran 2010)

Results: CMEs have a **complex structure** similar to a loop arcade system (Moran & Davila 2004), filaments around a single flux rope (Dere et al. 2005) → **flux rope structure not always present**. Erupting filament not centered within overlying envelope (Moran et al. 2010).

Limits: $\pm z$ ambiguity, only LOS mass-averaged z values, for COR1 H α 6563Å emission to be considered (Mierla et al. 2011).

Multiple view-points:

- **tie-pointing and triangulation:** identification of same structures by a) visual inspection (Liewer et al. 2009; Bemporad 2009), b) local correlation tracking (Gissot et al. 2008).
- **inverse modeling:** best underlying density reproducing observations (Antunes et al. 2009)
- **constraint on the mass calculation:** (Colaninno and Vourlidas, 2009)
- **forward modeling:** empirically defined model of a flux rope (graduated cylindrical shell - GCS) → synthetic tB – pB images (Chen et al. 2000; Thernisien et al. 2006; 2009)

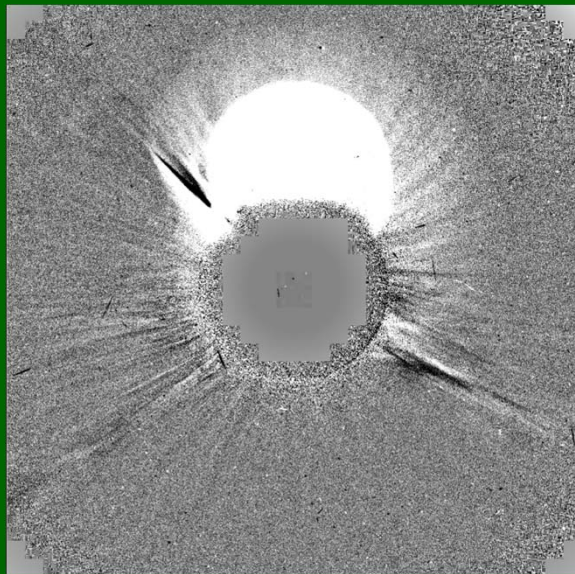
Results: majority of events reproduced by a “**hollow croissant**” model (Thernisien et al. 2009) surmounted by a hemispherical shell (Wood & Howard 2009) → CME+shock front (symmetric, radial, self-similar expansion). **CME masses (hence E_{kin}) underestimated** because of POS assumption (Vourlidas et al. 2000) and post-CME mass outflows (Vourlidas et al. 2010, 2011). **CMEs rotations** (Vourlidas et al. 2011, Bemporad et al. 2011), **deflections** (Kilpua et al. 2009, Lugaz et al. 2010), **interplanetary expansions** (Howard & Tappin 2010) measured in 3-D.

(see Mierla et al. 2010, Feng et al. 2012 for comparisons between various methods)

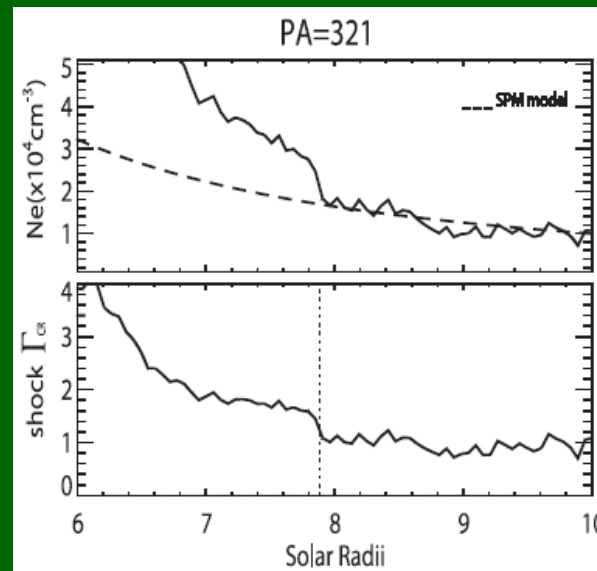
CME-driven shocks

Last 10 years: discovered that **WL images contain much more information** than previously thought → shock compression ratios, coronal fields, reconnection rates.

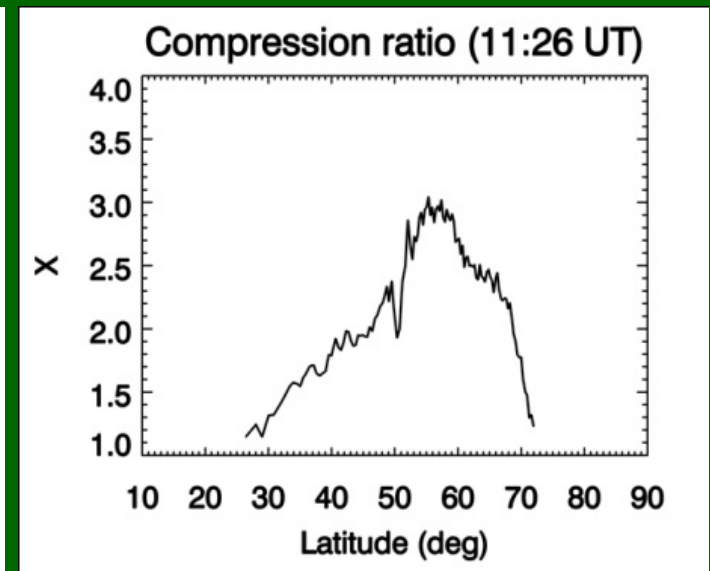
Fast CMEs ($v >$ local magnetosonic speed) drives coronal shock waves. For decades shocks were identified by remote sensing detection of a) streamer deflections, b) type-II radio bursts.



Vourlidas et al 2003



Ontiveros & Vourlidas 2009



Bemporad & Mancuso 2011

Results: compression ratios $X = \rho_d/\rho_u \sim 1.2-2.8$ at “**shock nose**”, density profiles consistent with “**3-D bow shock**” geometry (Ontiveros & Vourlidas 2009). Recently X derived all along the front of CME → **shock super- (sub-) critical at the nose (flanks)** (Bemporad & Mancuso 2011).

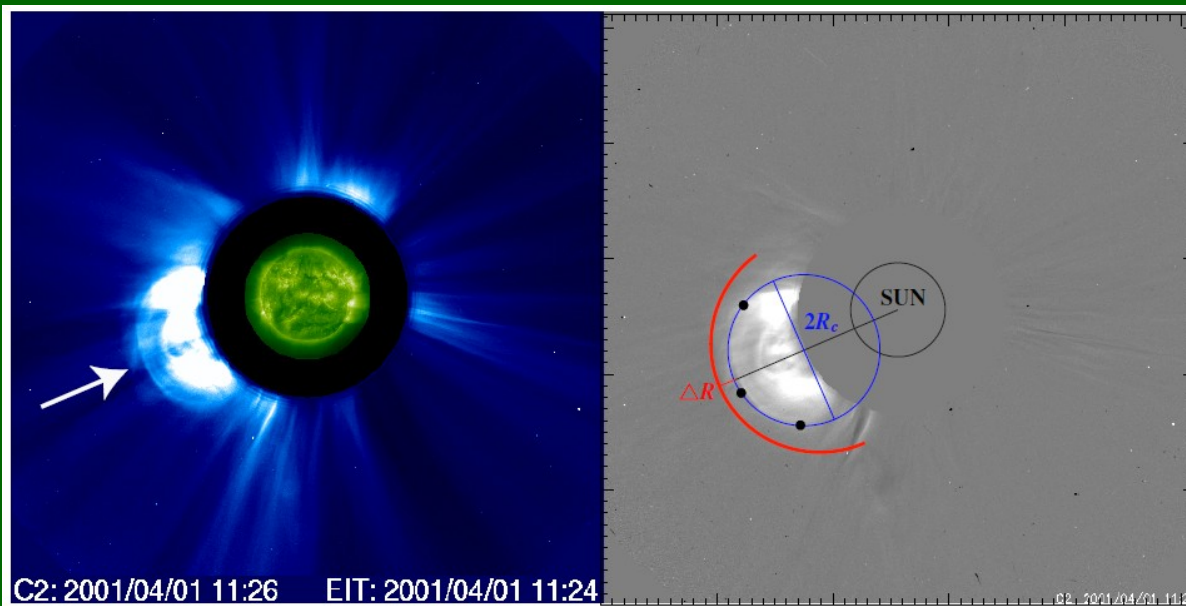
Limits: problems related with LOS integration (unknown LOS depth of structures, LOS density models need to be assumed).

Coronal magnetic field measurements

A new technique to **measure coronal fields crossed by CMEs** proposed by Gopalswamy & Yashiro (2011) by applying the Farris & Russell's (1994) relation between the standoff distance ΔR of an interplanetary shock and the radius of curvature R_c of the driver:

$$\frac{\Delta R}{R_c} = 0.81 \frac{(\gamma - 1)M^2 + 2}{(\gamma + 1)(M^2 - 1)}$$

$\Delta R = R_{shock} - R_{fluxrope}$, M = shock Mach number, γ adiabatic index.
Technique: measure R_{shock} and $R_{fluxrope}$ from WL images \rightarrow estimate of $M = v_{in}/v_A = (v_{shock} - v_{solarwind})/v_A \rightarrow$ measure v_{shock} and assume $v_{solarwind} \rightarrow$ estimate of $v_A = B/(\mu\rho)^{0.5} \rightarrow$ measure ρ (from pB images or type-II radio burst) \rightarrow **estimate of B .**



(Kim et al. 2012)

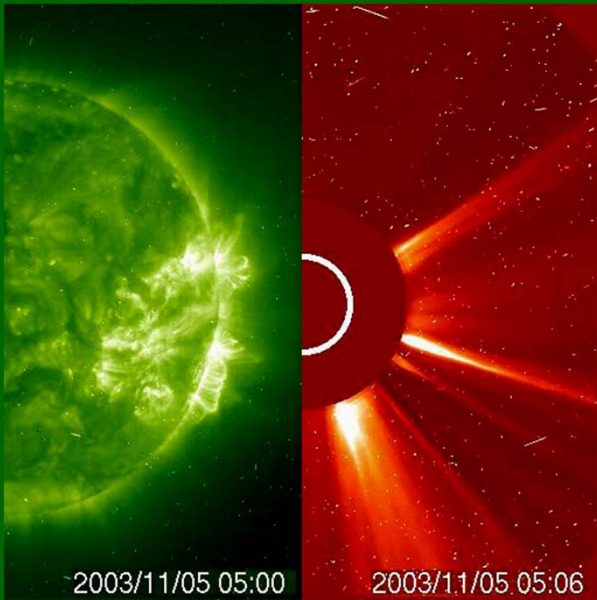
Results: B and v_A measured in a range between 3-15 R_{sun} , B consistent with previous measurements.

Shock **compression ratios X** from WL likely **underestimated** by a factor of ~ 2 because of LOS assumptions.

Limits: LOS integration effects

Recently applied by Gopalswamy et al. (2012) to a CME-driven shock observed in EUV with SDO/AIA.

Magnetic reconnection signatures



(Ciaravella & Raymond 2008)

Post-CME WL thin radial features interpreted as post-CME Current Sheets (Ko et al. 2003, Webb et al. 2003, 2004).

- observable only in $\sim 1/2$ of CMEs
- brighten ~ 4 hours after the CME
- observed sometimes within multiple ray-like structures
- $\sim 6 \times 10^4$ km thick, constant with time; lifetime ≥ 8 hours

Results: signatures of **bursty reconnection** (bi-directional flows & blobs along CS, inflows towards CS – Simnett 2004, Sheeley & Wang 2007, Vrsnak et al. 2009), $M_A = v_{in} / v_A \sim 0.01 - 0.2$ (Lin et al. 2005, 2007), $n_e \sim 10-100$ times > than corona, $T_e \sim 2-8$ times > than corona, CS cross section $\sim 10^5 \times 3.5 \cdot 10^4$ km² from 3-D reconstr. (Patsourakos & Vourlidas 2011).

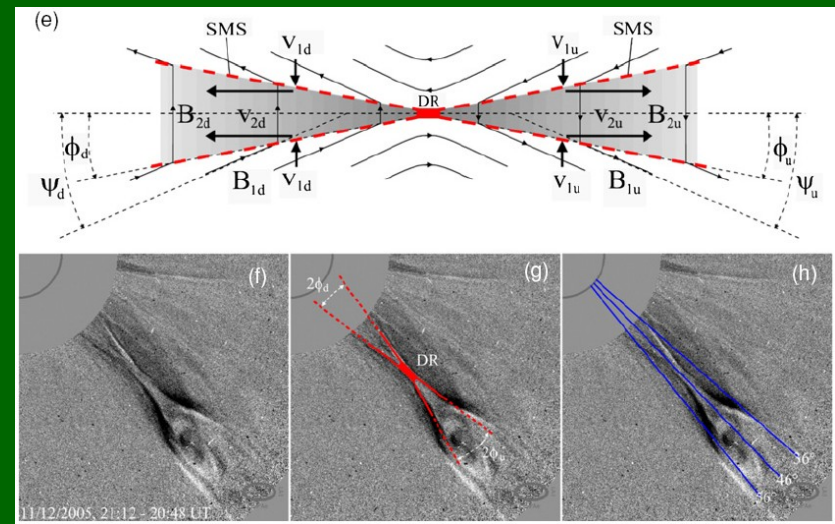
Information on magnetic reconnection also derived from white light images as

$$M_A = \frac{v_{in}}{v_A} \approx \frac{v_{in}}{v_{out}} = \frac{n_e(out)\delta}{n_e(in)\Delta} = X \tan(\phi)$$

X compression ratio across the SMS with angle 2ϕ .

Results: M_A decays with time/altitude

→ transition from fast Petschek-type to slow Sweet & Parker type reconnection? (Poletto et al. 2008, Bemporad et al. 2010).



(Bemporad et al. 2010)

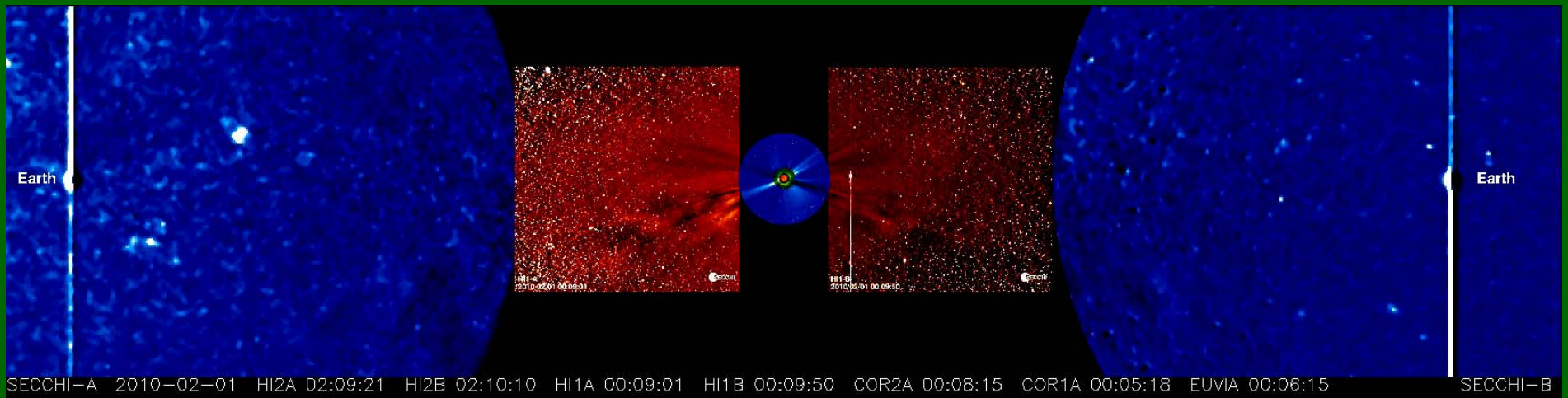
Interplanetary CME observations

SOLAR MASS EJECTION IMAGER
2008 TO SEPTEMBER 28, 2011

Interplanetary CMEs (**ICMEs**) are the primary cause of severe **space weather events** at Earth because they drive shocks and trigger geomagnetic storms that can damage spacecraft and ground-based systems.

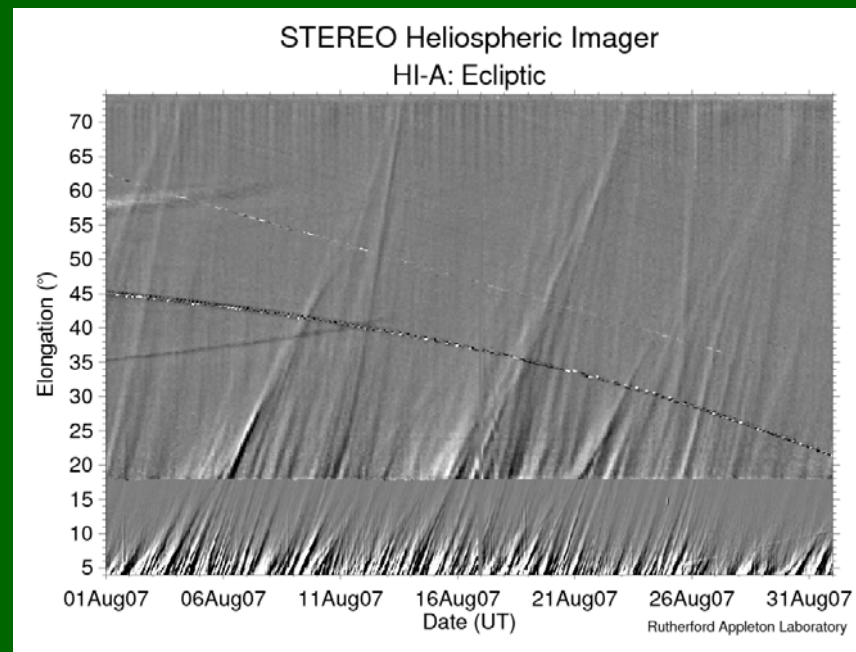
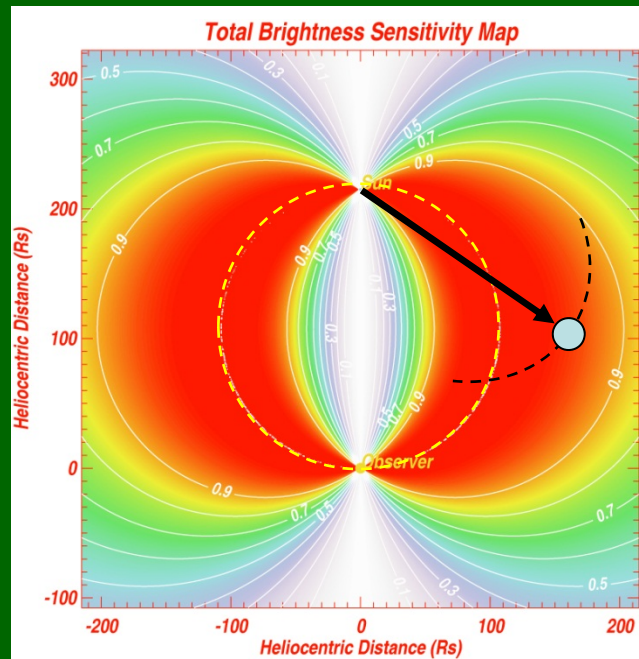
During the last decade ICMEs were imaged in white light by the **Solar Mass Ejection Imager** (SMEI, 2003-2011) → observed more than ~400 ICMEs (Webb et al. 2006; Howard & Simnett 2008).

More recently ICMEs observed by the **SECCHI/Heliospheric Imagers** (HI1-HI2) onboard twin STEREO spacecraft (2006-now; Howard et al. 2008).



Interplanetary CME observations

(courtesy of A. Vourlidas)



WL emission maximizes over the **Thompson sphere** (Vourlidas & Howard 2006).

Heliospheric observations of ICMEs are used for their tracking (J-maps), space weather forecastings, and 3-D reconstructions (combined with in situ data).

Many techniques have been developed to provide **propagation direction and velocity of ICMEs** from HI observations both from single and multiple viewpoints (e.g. Rouillard *et al.*, 2008, 2009, 2010; Lugaz *et al.*, 2010; Liu *et al.*, 2010).

Results: heliospheric appearance of ICMEs depends also on their interaction with background wind and internal evolution → significant alterations of flux rope topologies likely occur leading to formation of **multiple propagating density structures**. Predicted arrival times at Earth have easily errors around ~ 6-11 hrs.

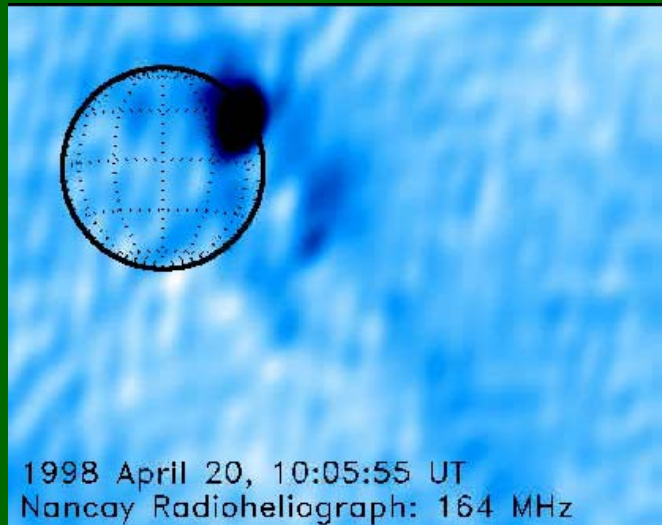
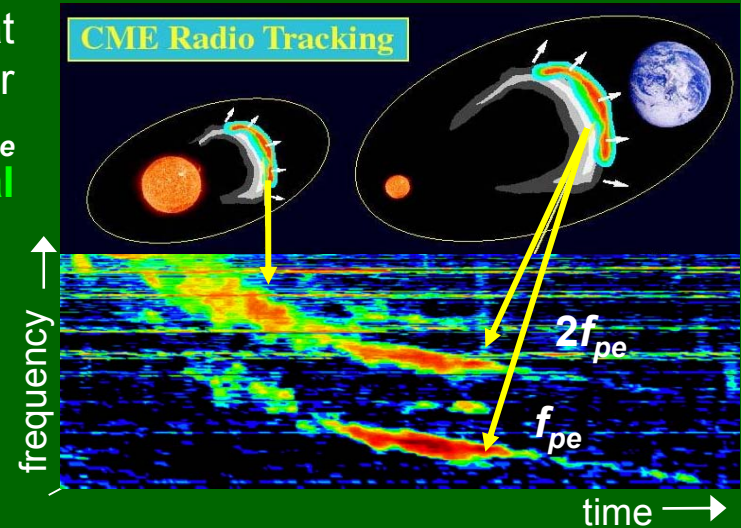
Radio observations

CME radio emission

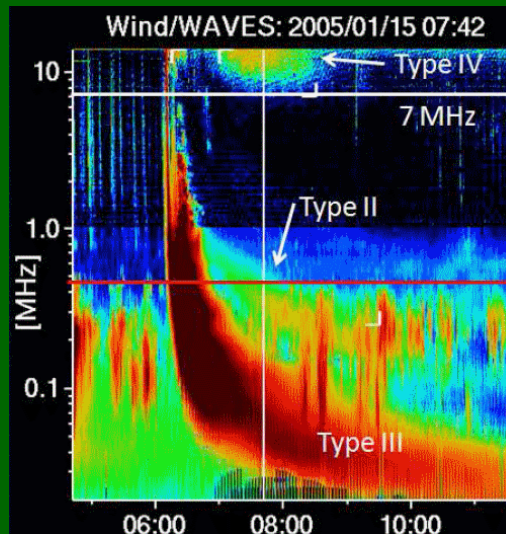
Flares/CMEs drive **shocks** accelerating SEPs and non-thermal e^- beams (~ 10 keV) generating **plasma waves** at the local plasma frequency f_{pe} that scatter off ions or combine to produce **type II radio emission** at f_{pe} (**fundamental**) and $2f_{pe}$ (**harmonic**) \rightarrow **non-thermal plasma emission**.

$$f \approx f_{pe} \equiv \sqrt{\frac{e^2 n_e}{m_e \pi}} \propto \sqrt{n_e}$$

Type IIs offer evidence of coronal shocks but 1) no spatial resolution/imaging of shock, 2) little information on **physical properties of shocked plasma** (only n_e)



(Bastian et al. 2001)



(Gopalswamy 2001)

CMEs associated also with:

- **type-IIs** (e^- beams accelerated along open fieldlines)
- **type-IV** (e^- accelerated and trapped in low corona in closed fieldlines)

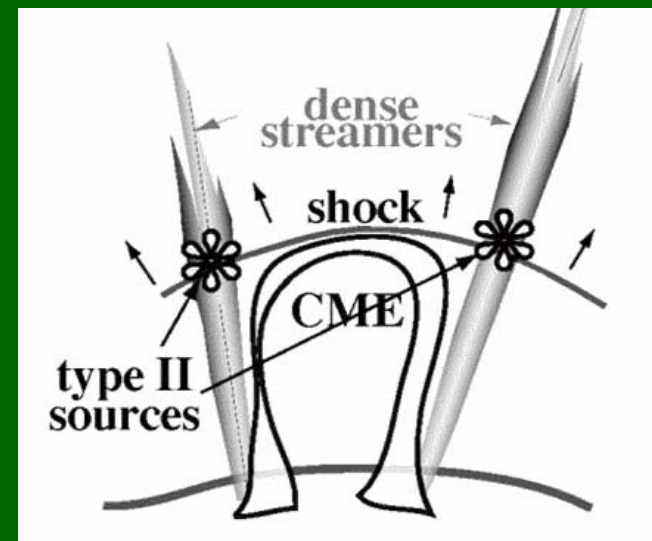
Radio images of CMEs:
thermal free-free (Sheridan 1978, Gopalswamy & Kundu 1992) and **non-thermal gyrosynchrotron** (Hildner 1987, Bastian et al. 2001).

CME radio observations: some results

SOHO WL vs radio: multiple loop systems rapidly (5-15 min) involved (Maia et al. 1998, 1999; Pick et al. 1998). Previous associations (Cane et al. 1987) of metric **type-II bursts with CMEs-driven shocks confirmed** (Cliver et al. 1999, Maia et al. 2000, Reiner et al. 2003). Type IIs originate in regions along the shock front of higher than normal densities (e.g. streamers – Reiner et al. 1998). M-DH type-II come from shock flanks, DH-km come from shock nose (Raymond et al., 2000).

Statistical studies: “Radio-loud CMEs” (i.e. with type IIs) statistically faster, wider and associated with stronger flares than “radio-quiet CMEs”, but slow ($v \ll 900$ km/s) RL-CMEs & fast ($v \gg 900$ km/s) RQ-CMEs also observed → surrounding coronal conditions (Gopalswamy et al. 2008).

STEREO WL vs radio: type-IIs form when the CME is between **1.5 and 3-4 R_{sun}** (v_A locals min & max – Warmuth & Mann 2005) (Gopalswamy et al. 2009; Ramesh et al. 2012). Very close **associations** between the **CME nose** and the **DH-km type-II** and between **CME-streamer** interaction and the **m-DH type-II** burst (Cho et al. 2011).

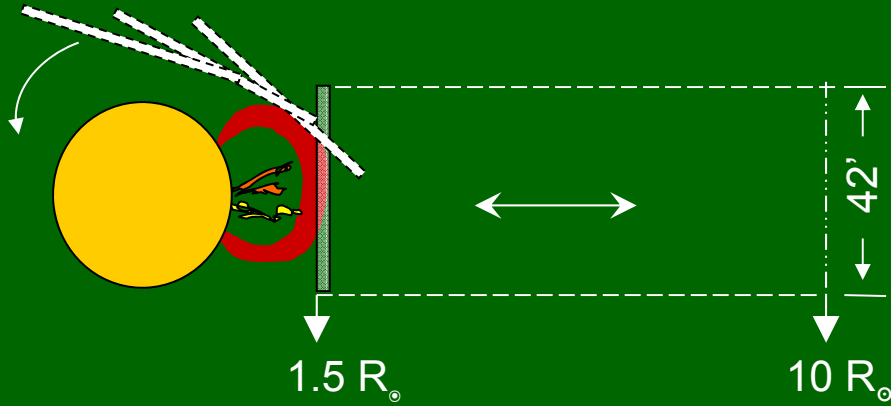


(Reiner et al. 2003)

UV observations

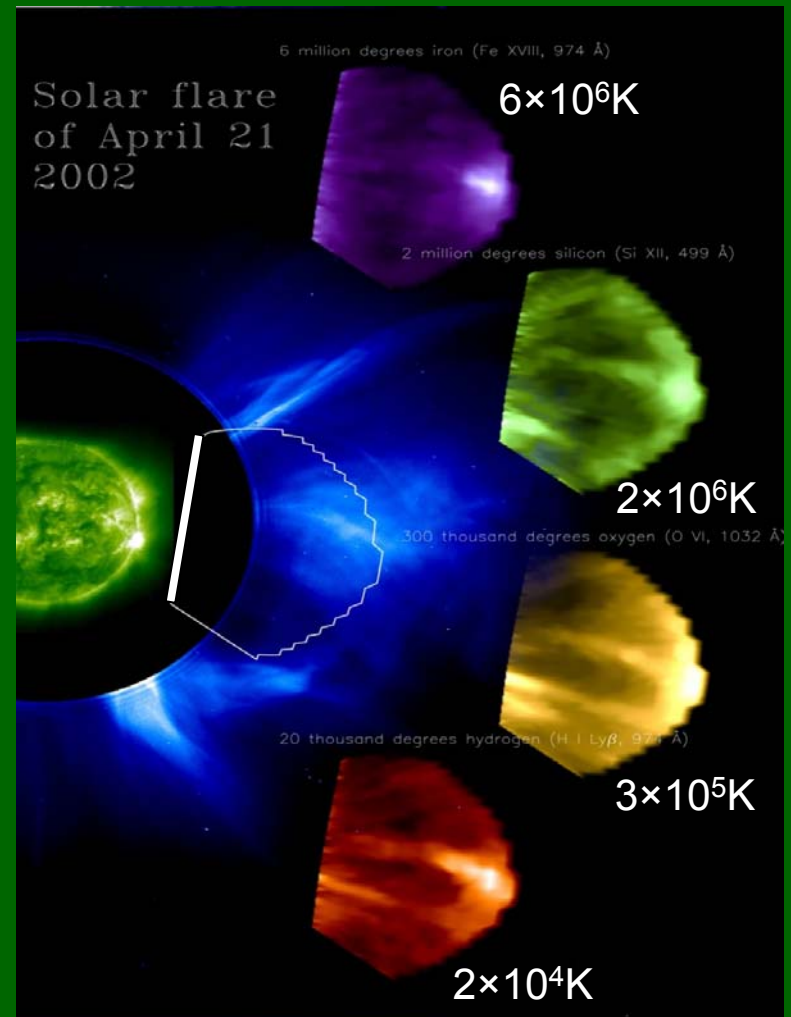
SOHO UV Coronagraph Spectrometer

UVCS FOV: entrance slit 42' long and up to 84" wide, can be pointed at any polar angle and heliocentric distance from 1.5 to 10 R_{\odot} .



2 UV spectrometers: HI Ly- α and OVI channels → emission lines in the 950–1350 Å range, spatial resolution 7"/pixel (0.01 R_{\odot}), spectral resolution ~ 0.1 Å/pixel (Kohl et al. 1995).

CMEs observed by UVCS typically with exposure times by 100-200s and spatial resolutions by 21"-70"/pixel (see Kohl et al. 2006 for a review)



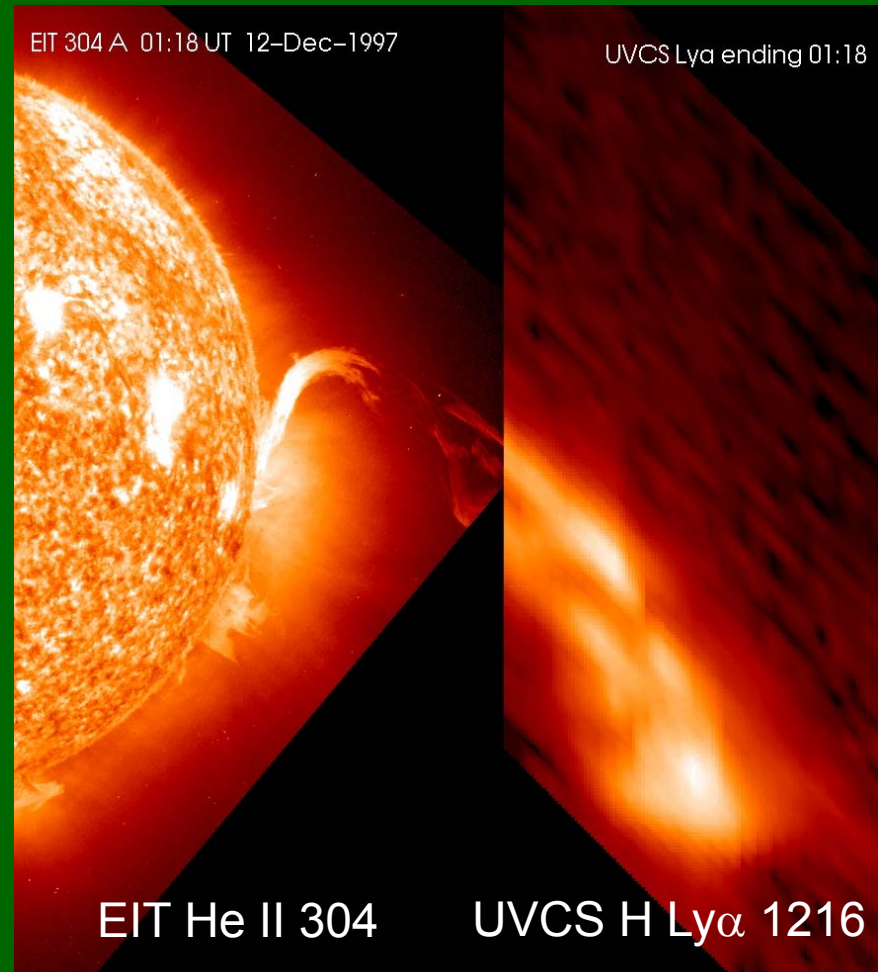
(Raymond et al. 2009)

CME properties from UVCS (1)

CME CORE:

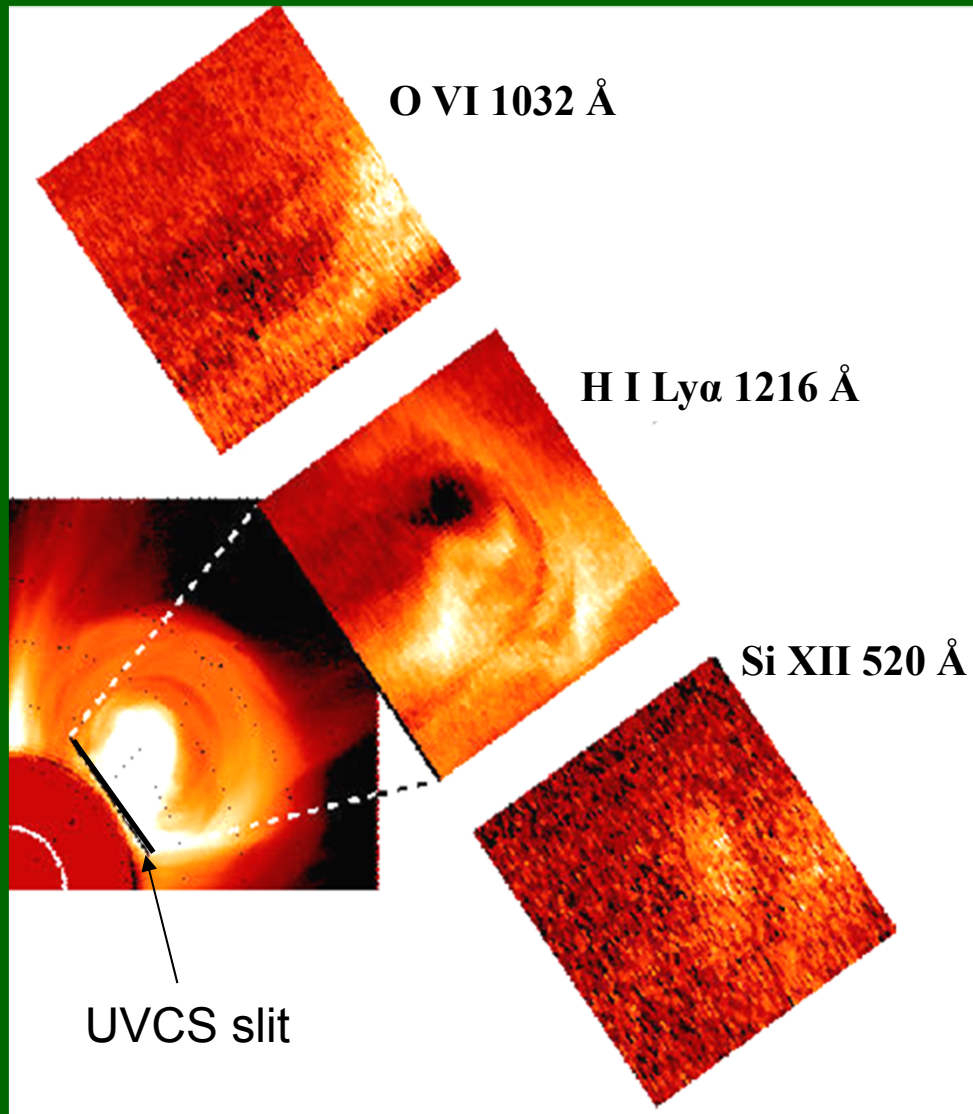
Many different features: **single** bright “cool” emitting **knots** (Ciaravella et al. 1999); **many bright knots** or spots with different velocities → “different, isolated CME structures” (Ventura et al. 2002); S-shaped configurations → **helical topologies** (Ciaravella et al. 2003); rotation of velocity vector associated with **helical motions** of plasma (Antonucci et al. 1997).

Handedness of helical expanding features in agreement with pre-CME filaments. Usually lines from “cool” ($10^{4.6} \text{ K} < T < 10^{5.5} \text{ K}$) ions observed (e.g. C III, Si III). **Continuous heating** at the CME core is required to match some UVCS observations (Bemporad et al. 2007; Lee et al. 2009; Landi et al. 2010 – **see later**).



(Ciaravella et al. 2000)

CME properties from UVCS (2)



(Ciaravella et al 2003)

CME VOID:

- Density depleted region, difficult to analyze.
- Void temperatures are likely larger than pre-CME corona (Ciaravella et al. 2003, Bemporad et al. 2007)

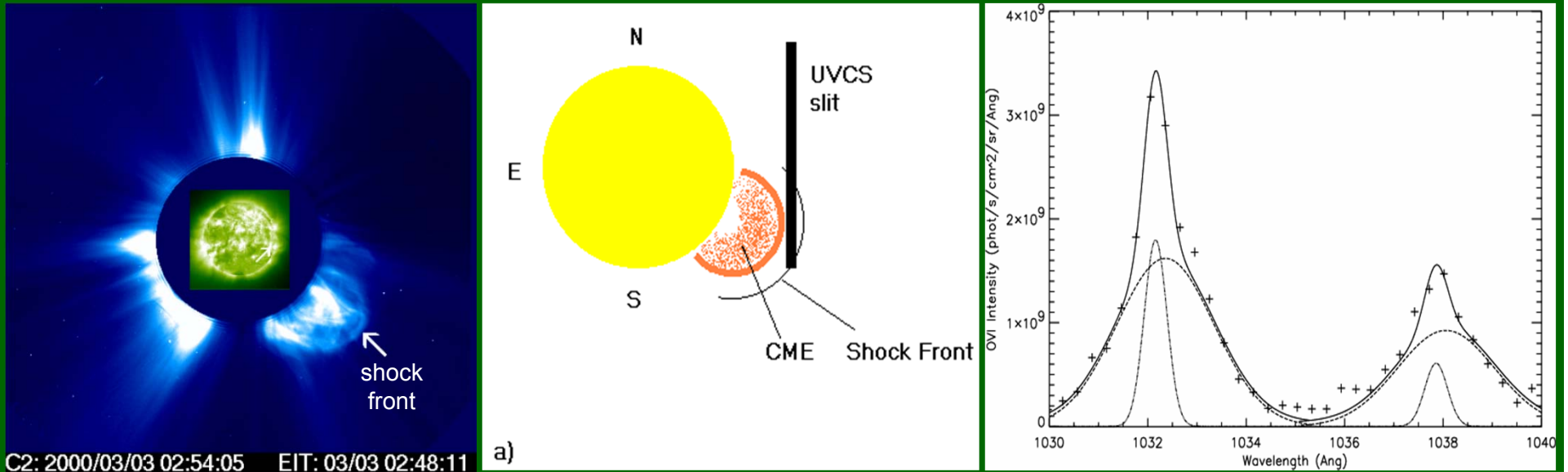
CME FRONT:

- Slow CMEs: in some events front plasma is **denser and cooler** than surrounding coronal structures (e.g. Ciaravella et al. 2003), other events signatures of **adiabatic compression heating** (Bemporad et al. 2007).

CME-DRIVEN SHOCK:

- Fast CMEs: signatures of **shock heating** in line profiles (e.g. Mancuso et al. 2000)

CME-driven shocks (1)



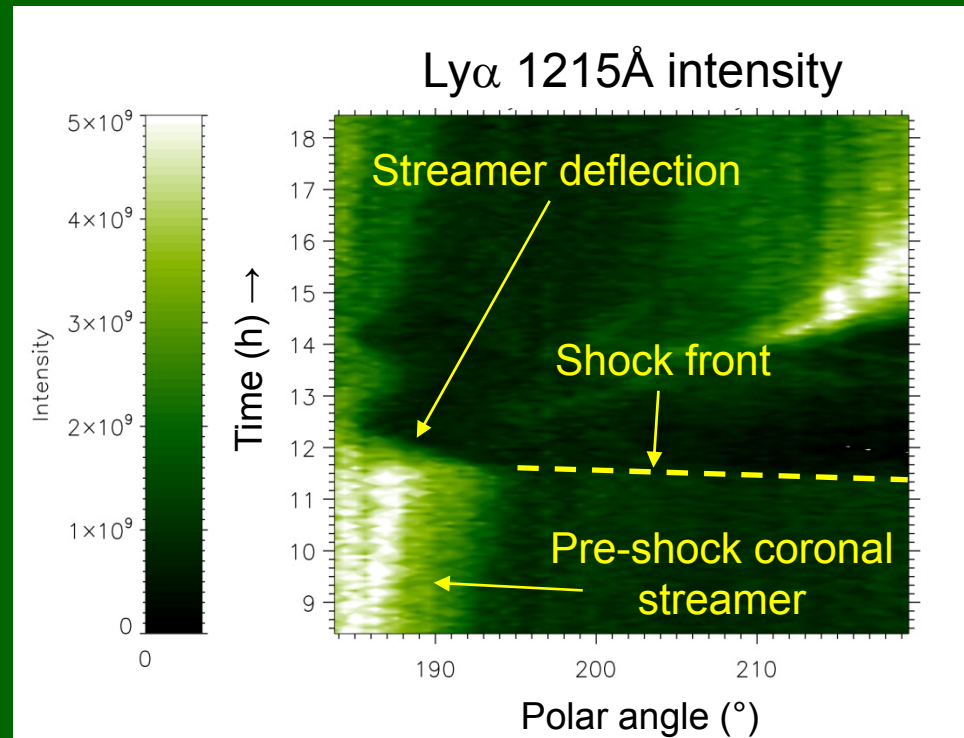
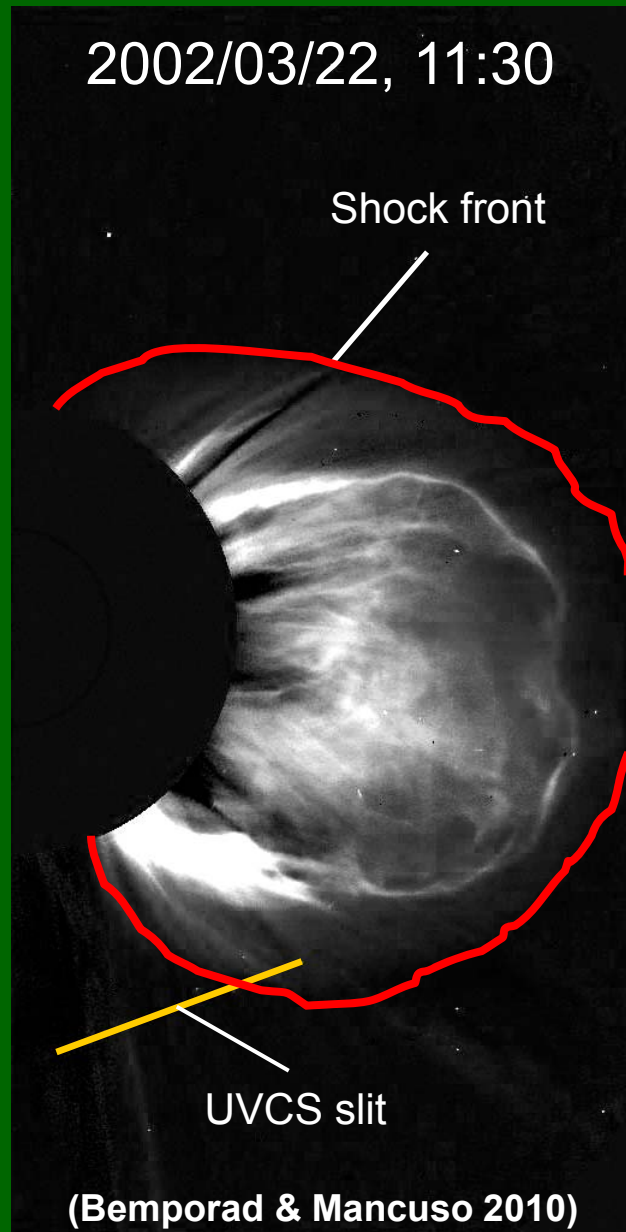
Broad wings in the O VI doublet (right) as results of a shock passage (left; from Mancuso et al. 2000, A&A).

The **passage of a shock** heats the emitting material and is detected as **broad wings** mainly in the non neutral ions (associated with type-II radio bursts). In the UVCS spectra the **presence of a shock front** is more likely detected in the brightest spectral lines such as the **O VI doublet** and the **H I Ly- α line**, providing a direct diagnostic of the kinetic temperatures behind the shock.

Detections of five shocks in UV spectra reported so far (Raymond et al 2000; Mancuso et al. 2002; Raouafi et al. 2004; Ciaravella et al. 2005; Mancuso & Avetta 2008; Bemporad & Mancuso 2010).

Shocked plasma: high O⁺⁵ ion kinetic temperature ($T_k \sim 10^8$ K) and smaller electron temperature ($T_e \sim 10^7$ K). Comparison with timing of radio data suggests that type-II burst originate likely at the CME shock front (e.g. Mancuso et al. 2002).

CME-driven shocks (2)



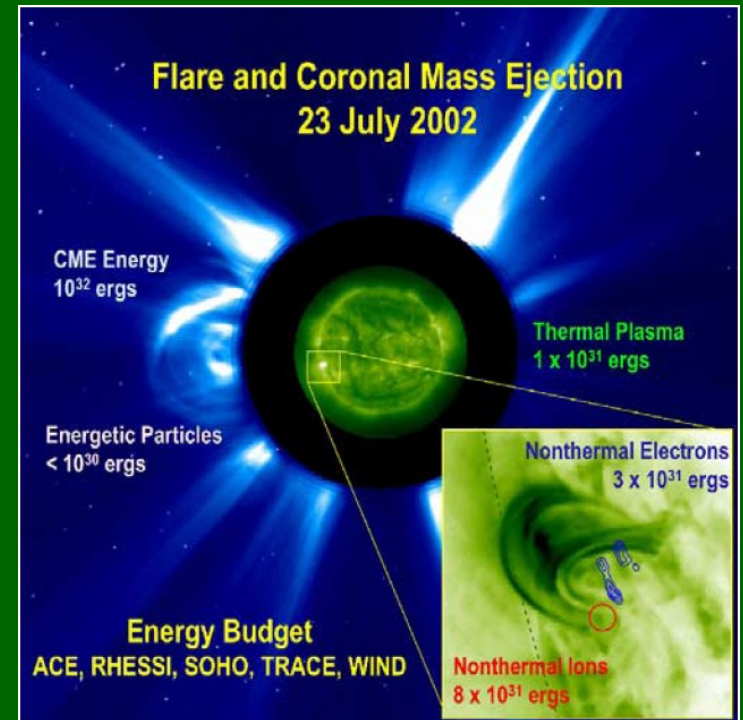
- Fast CME, X-class flare and type-II burst.
- LASCO, UVCS → upstream parameters, but the field.
- upstream parameters from UV + compression ratio X from WL → R-H equations → downstream params.
- **Shock** → 1) plasma compression (~ 2.06), 2) heating (by a factor ~ 8) 3) B compression from 0.02G to 0.04 G, 4) magnetic & kinetic energy increases comparable

Shows the potential of combining WL and UV data!

CME energy partition (1)

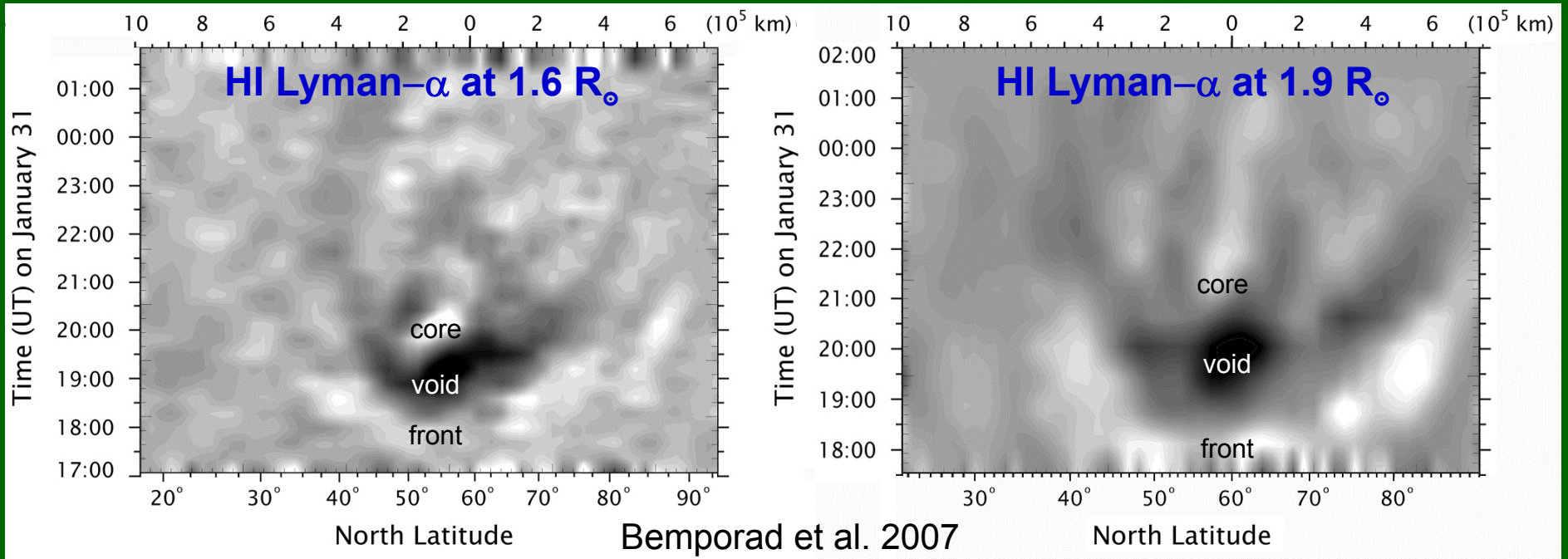
UVCS observations constrained the heating rates in the cores of a CMEs:

- **Akmal et al. (2001)**: substantial heating must be added as the plasma expands to maintain the observed T. **Total heating comparable to CME kinetic and gravitational potential energies** (agreement with prediction by Kumar & Rust (1996) model) → should be considered in CME models.
- **Lee et al. (2009)**: continuous heating required to match UVCS obs., **heating energy greater than the kinetic energy**. Different heating rates are required for bright knots; ~75% of magnetic energy goes into the heating energy.
- **Landi et al. (2010)**: **total heating several times larger than kinetic energy**. Wave heating, thermal conduction, and internal shocks (Filippov & Koutchmy 2002) cannot supply required heating. **Magnetic heating, shocks** generated by outflows from the reconnection region, and **energetic particles** from reconnection region are viable heating mechanisms.



Majority of ejected energy assumes the form of mechanical energy carried by the CME (e.g. Emslie et al. 2004, 2005)?

CME energy partition (2)



Study of CME thermal energy evolution \rightarrow need that UVCS observes the **SAME event at different h** (like a **multislit spectrometer**). A very few ($\sim 3-4$) slow CMEs observed by UVCS alternatively at 2 different altitudes. Only one of these studied.

Results (combining WL and UV data): front hotter than corona, **heating compatible with adiabatic compression**. T_e larger by $\sim 40\%$ in the core than in the front \rightarrow additional heating source at the core. T_e increases by $\sim 10\%$ between 1.6 and 1.9 solar radii \rightarrow **conversion of magnetic to thermal energy during expansion?**

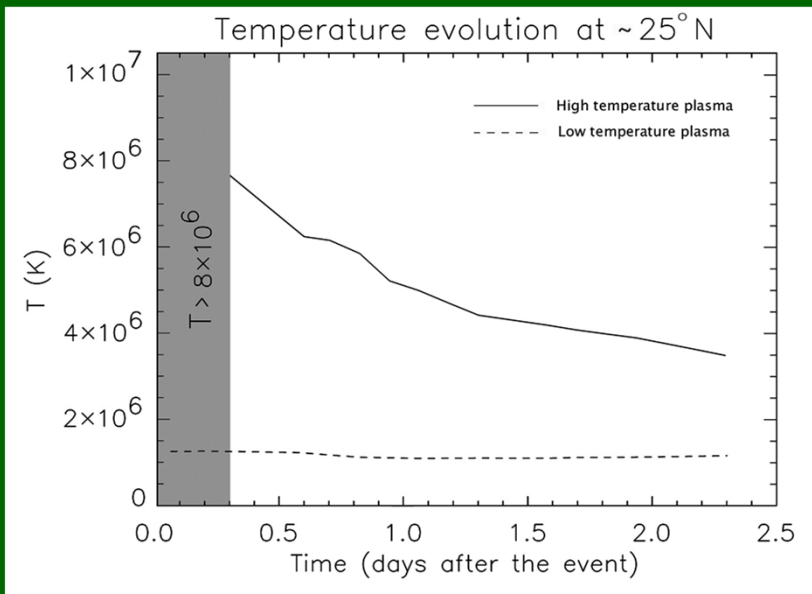
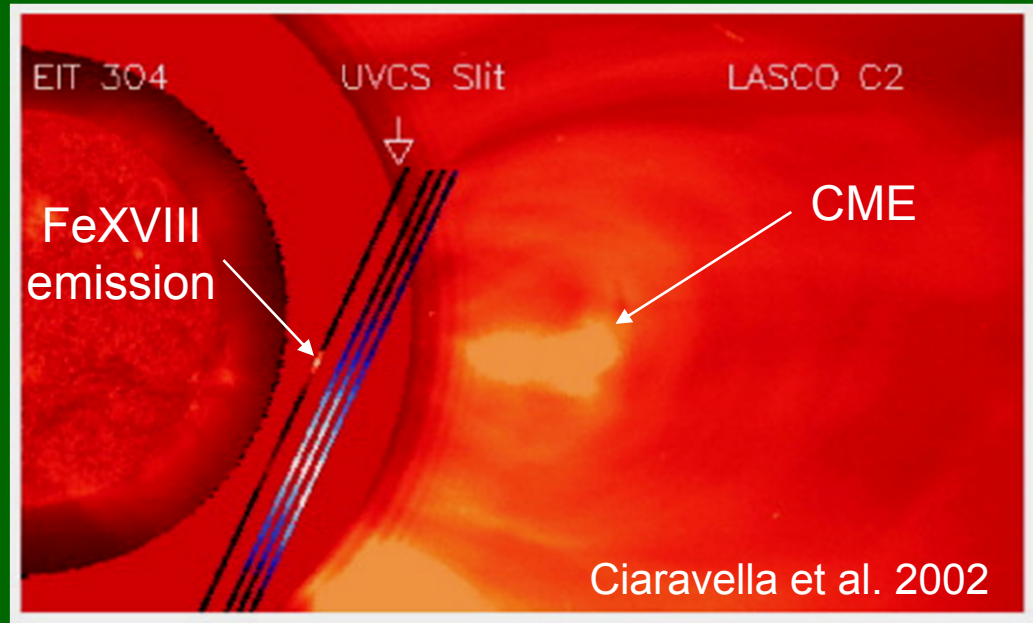
Shows potential of combining WL and UV data and «multi-slit» studies of CME

Post-CME current sheets (1)

UVCS observations:

Strong **Fe XVIII emission** → CS plasma at high T ($\sim 5 \times 10^6$ K)

- CS have long (\sim days) lifetime
- Elemental abundances similar to those of ambient corona (FIP effect) → CS material brought in from its sides (Ko et al., 2003; Lin et al. 2005, Ciaravella & Raymond 2008)



(Bemporad et al. 2006)

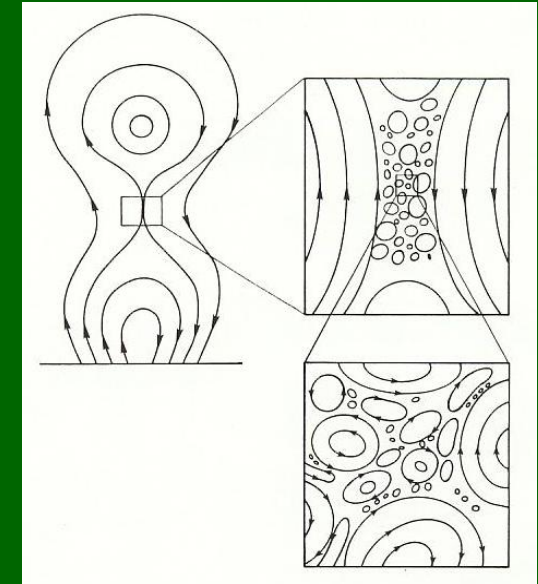
In a unique dataset post-CME CS observed continuously for ~ 2.3 days → evolution of CS physical parameters derived for the first time. **Adiabatic compression** explains the large CS temperatures only at the end of observations (Bemporad et al. 2006).

FeXVIII 974Å profile evolution → first study of **plasma turbulence** in a post-CME CS.

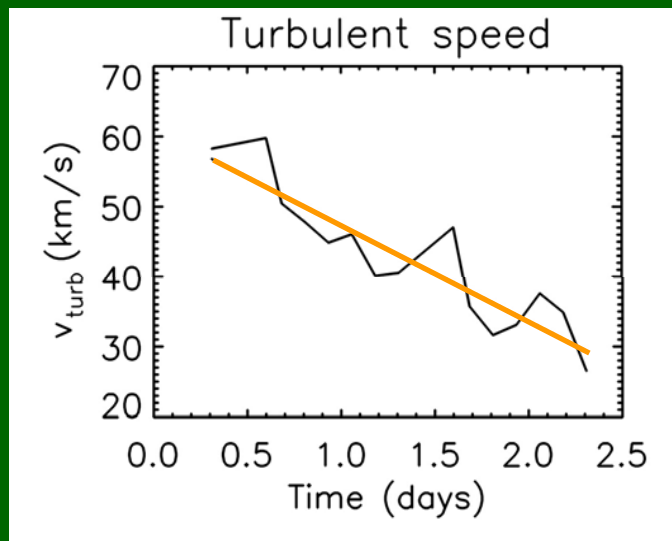
Post-CME current sheets (2)

Plasma turbulence inside CS could explain the long persistence, huge thickness and large temperature of CSs. Its development is expected because of:

- 1) **Macroscopic instabilities** (e.g. tearing - Tajima & Shibata 1997) in the elongated post-CME CS;
- 2) **Microscopic instabilities** (e.g. current aligned - Silin & Buechner 2003, Daughton et al. 2004)



Development of a fractal CS (Tajima & Shibata)



Result: continuous decrease of $v_{turb} \sim 60$ km/s to ~ 30 km/s (Bemporad 2008)

Multiple small-scale (10 - 10^4 m) reconnections explain:

1) **high CS temperatures** (adiabatic compression + mag. reconnection).

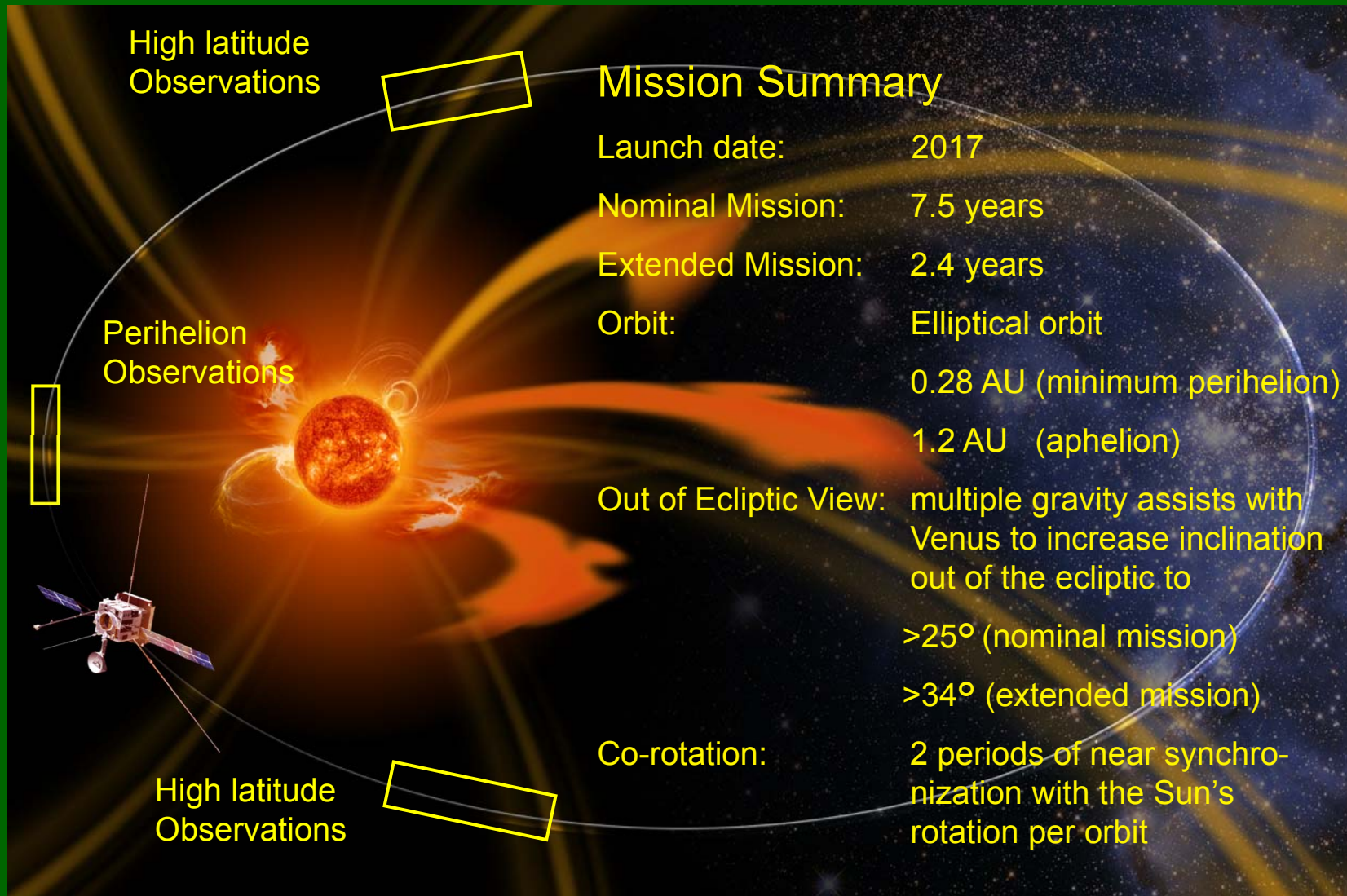
2) **pressure balance** between coronal and CS plasma (needed to explain the stationarity of CS)

3) **large observed thickness** of CS (broadened by turbulence – Lazarian & Vishniac 1999).

OPEN QUESTION: reconnection in HXR often observed by RHESSI (Saint-Hilaire 2009) is an alternative heating source?

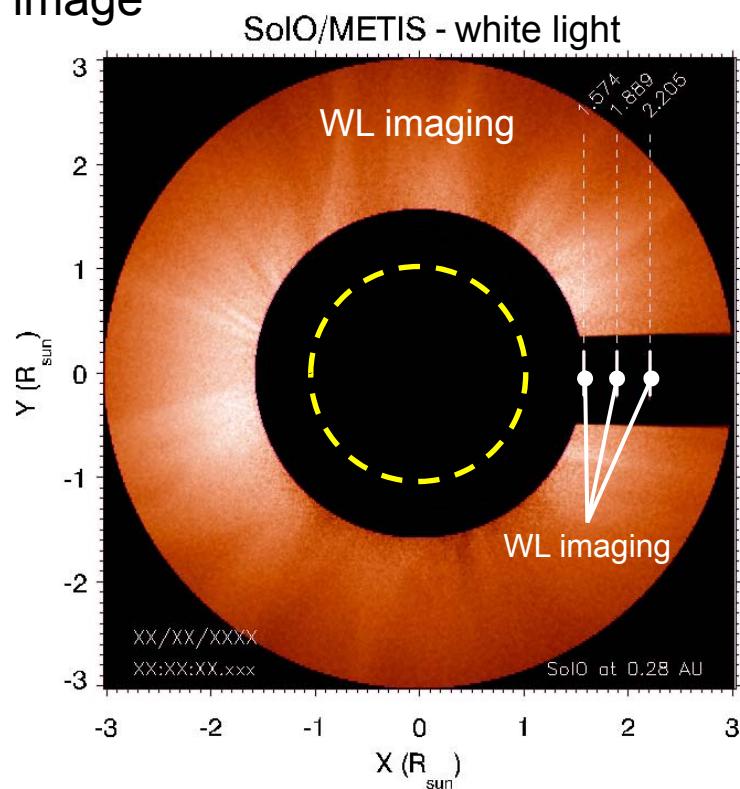
The Future

Development of new instrumentation e.g.: Solar Orbiter Mission

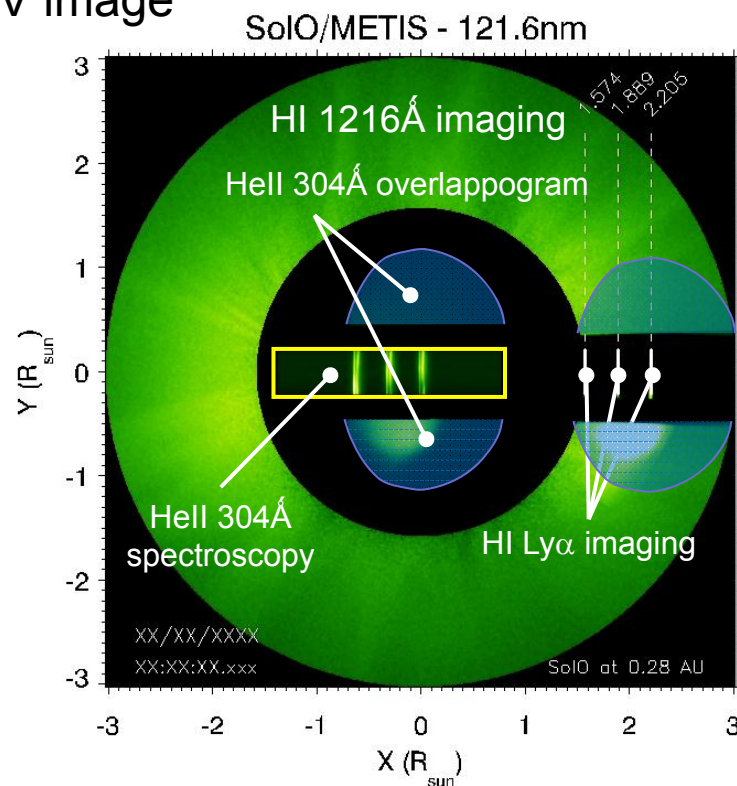


METIS: Multi Element Telescope for Imaging & Spectroscopy

WL image



EUV image



METIS FOV:

Imaging channel FOV: annular, $1.5^\circ - 2.9^\circ$
 Spectrosc.channel FOV: 3 slits at $1.5^\circ, 1.8^\circ, 2.1^\circ$
 each slit is 0.4° long
 Spectral resolution: $0.0675 \text{ \AA}/\text{pixel}$ in the 304 \AA channel

METIS FOV at 0.28 AU:

annular, $1.57 - 3.05 R_{\text{sun}}$
 3 slits at $1.57, 1.89, 2.21 R_{\text{sun}}$
 each slit is $0.42 R_{\text{sun}}$ long

METIS FOV at 0.70 AU:

annular, $3.94 - 7.62 R_{\text{sun}}$
 3 slits at $3.94, 4.72, 5.51 R_{\text{sun}}$
 each slit is $1.05 R_{\text{sun}}$ long



Development of new simulation capabilities e.g.: SWIFF project



SWIFF (Space Weather Integrated Forecasting Framework) is a European Commission project funded by ERC 7th Framework Programme.
Kick-off: February 2011 – Project's end: January 2014.



Working Package Leaders:

Lapenta Gianni, PI – WP1 (K.U. Leuven, Be);
Keppens Rony, WP2 (K.U. Leuven, Be);
Nordlund Per-Ake, WP3 (UCPH Copenhagen Univ., Denmark);
Califano Francesco, WP4 (UniPi Pisa Univ., It);
Pierrad Viviane, WP5 (BISA, Institute d'Aeronomie Spatiale, Brussels, Be);

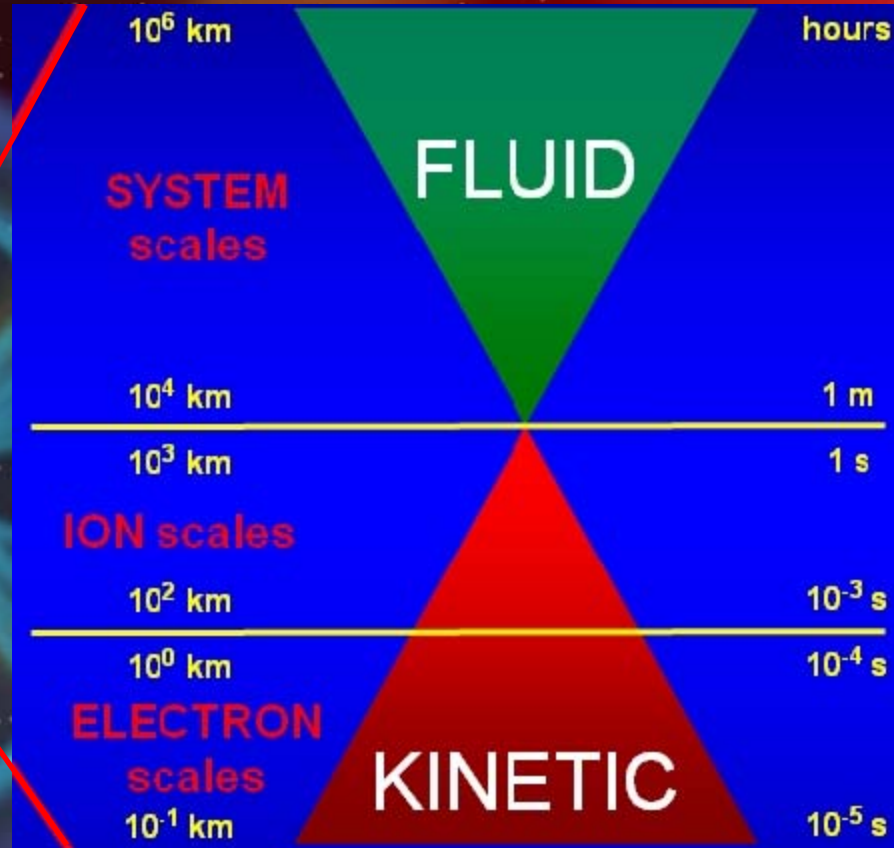
Other Institutes involved:

INAF-OATo (Turin Astrophysical Observatory, It)
ASI (Czech Republic Astronomical Inst., Cz)
USTAN (Univ. of St. Andrews, UK)

www.swiff.eu/wiki



SWIFF activities



WP5
coupling at the
Earth

WP4
solar wind
interaction with
magnetosphere

WP2
multi-physics
software tools

WP3
coupling at the
Sun's surface

Summary & Conclusions

- **Radio, WL and UV observations** of CMEs in the **outer corona** provided a lot of information **not only on CME** themselves, but also on many **related phenomena** like post-CME CS, CME-driven shocks, CME induced reconnections, CME energy partition, etc...
- Many significant results were obtained only when **data from completely different spectral windows were combined** (radio & WL or WL & UV data).
- Many results on interplanetary propagation of CMEs were obtained only when **data from remote sensing and in situ instruments were combined**.
- **Merging of different expertises** will be really important for future understanding of open problems on CMEs.
- **Future development of new instrumentation and new simulation capabilities** will be also crucial.